Ratnakumar, 2021, 9:6
ISSN (Online): 2348-4098
ISSN (Print): 2395-4752

Reaction Kinetics of Various Oxygen Carriers in Chemical Looping Combustion Using Methane as Fuel

Research Scholar RatnaKumar V. Kappagantula, Lecturer Gordon D. Ingram,
Associate Prof. Hari B. Vuthaluru,
Department of Chemical Engineering,
Curtin University, Bentley Campus,
Western Australia, Australia.
v.kappagantula@postgrad.curtin.edu.au, g.ingram@curtin.edu.au, H.Vuthaluru@curtin.edu.au

Abstract- Chemical Looping Combustion is the latest technology with a distinct benefit from carbon dioxide's inherent separation from Nitrogen. This separation is not possible in conventional fossil fuel-fired boilers, which requires higher energy demand. HSC Chemistry software V 10.0 is used to evaluate the thermodynamic data. The obtained thermodynamic data is validated with published literature for log (K) and 1/T values. The sum of the heat of the Fuel Reactor and the Air Reactor reactions is the same as the heat generated from fuel combustion in a conventional boiler. The Reduction in the Fuel Reactor is endothermic except for all Copper-based and a few Manganese-based redox pairs. Reactivity data for various types of Oxygen Carrier pairs with methane are presented and discussed for use in a Fuel Reactor of Chemical Looping system. The minimum theoretical temperature required for different Oxygen Carrier to be reduced by methane is analyzed. The activation energy for sixteen redox pairs is investigated and categorized from higher to lower activation energy. The Copper-based Oxygen Carrier requires less activation energy compared to other redox pairs. The Oxygen Carrier particles are categorized based on their ability to transfer Oxygen and the maximum extent of conversion. A pair of Manganese and Iron have higher Oxygen transport capacities. The sum of heat of reactions to the difference in mass of reduced and oxidized Oxygen Carrier is constant. The cost of the metal for Oxygen Carrier is analyzed, and iron ore and Manganese are the economical options. The advantages and disadvantages of selected Oxygen Carriers are presented.

Keywords: Chemical Looping Combustion, Oxygen Carrier, Cost, and Activation Energy etc.

I. INTRODUCTION

Chemical Looping Combustion is the latest technology with a distinct benefit from carbon dioxide's inherent separation from Nitrogen. This separation is not possible in conventional fossil fuel-fired boilers, which requires higher energy demand. HSC Chemistry software V 10.0 is used to evaluate the thermodynamic data. The obtained thermodynamic data is validated with published literature for log (K) and 1/T values. The sum of the heat of the Fuel Reactor and the Air Reactor reactions is the same as the heat generated from fuel combustion in a conventional boiler. The Reduction in the Fuel Reactor is endothermic except for all Copper-based and a few Manganese-based redox pairs.

Reactivity data for various types of Oxygen Carrier pairs with methane are presented and discussed for use in a Fuel Reactor of Chemical Looping system. The minimum theoretical temperature required for different Oxygen Carrier to be reduced by methane is analyzed. The activation energy for sixteen redox pairs is investigated and categorized from higher to lower activation energy. The Copper-based Oxygen Carrier requires less activation energy compared to other redox pairs. The Oxygen Carrier particles are categorized based on their ability to transfer Oxygen and the maximum extent of conversion.

A pair of Manganese and Iron has higher Oxygen transport capacities. The sum of heat of reactions to the difference in mass of reduced and oxidized Oxygen Carrier is constant. The cost of the metal for Oxygen Carrier is analyzed, and iron ore and Manganese are the economical options. The advantages and disadvantages of selected Oxygen Carriers are presented.

In the boilers operating on fossil fuel combustion, combustion occurs at the combustion chamber with combustion air. The products of the combustion are carbon dioxide (CO_2), water vapour (H_2O), Nitrogen (N_2) and un-reacted Oxygen (O_2). Usually, the composition of O_2 in the flue gas is about 2%.

The heat generated during the combustion is used in heating the BFW to saturation temperature, evaporating BFW at a constant temperature to make saturated steam and superheating steam to the superheated temperature. The separation of CO_2 from other flue gas components incurs a significant energy penalty. Therefore, it is required to find an alternative solution to separate CO_2 from N_2 without affecting the combustion process.

The current technologies are

- Use of pre-combustion technologies for the pre-combustion decarburization of fuels.
- The oxyfuel combustion method separates O_2 from the air and substitutes the air in the furnaces with O_2.
- Post-combustion systems use solvents to remove CO_2 from other components in the flue gas treatment.

1. Chemical Looping Combustion:

Existing CO_2 removal technologies are expensive and appreciably increase electricity consumption and heat release [1]. The search for an alternative technology to capture CO_2economically and efficiently led to several kinds of research. Chemical Looping Combustion (CLC) is a novel technology with inherent CO_2 capture ability and higher energy efficiency than other prevailing CO_2 capture technologies [2].

In the CLC process, Fuel reacts with a metal oxide in the Fuel Reactor (FR). The metal oxide is reduced to metal. Simultaneously, the Fuel reacts with the O_2 from the metal oxide to produce CO_2 and H_2O as the flue gas. Water is separated from the flue gas stream after heat recovery. The metal from the FR passes on to the Air Reactor (AR).

In the AR, the metal is oxidized to the metal oxide by reacting with the O_2 from the air. The O_2-depleted air exits the AR for heat recovery, and the metal oxide is returned to the FR. The recycled metal/metal oxide is the Oxygen Carrier (OC) transported on an inert support material.

The reaction in the FR for any metal oxide OC is

$$(2m+n)Me_xO_y + C_mH_{2n} \rightarrow (2m+n)Me_xO_{y-1} + mCO_2 + nH_2O \quad \textbf{(1)}$$

The reaction in the AR is

$$Me_xO_{y-1} + \frac{1}{2}O_2 \rightarrow Me_xO_y \quad \textbf{(2)}$$

A simplified diagram of CLC is presented in Fig, in which the Fuel is CH_4 and the redox pair is hematite/magnetite (Fe_2O_3 / Fe_3O_4).

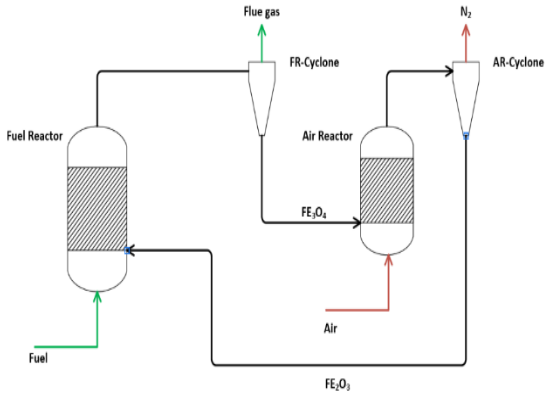

Fig 1. Basic diagram of CLC process.

2. Oxygen Carrier:

Between FR and AR, the OC circulates and releases O_2 for FR combustion. The reduced OC then re-circulates to AR, where the OC would be re-oxidized to its oxide form.

The characteristics of the OC are[3]

- Good O_2 carrying capacity
- A good gas reaction in oxidation and reduction reactions.
- High rates of reactions
- Good long-term recyclability and durability.
- Good mechanical strength.
- Suitable heat capacity and high melting point.
- Ability to change the heat of reaction.
- Low cost and ease in scaleup of the synthesis process.
- Suitable particle size.
- Resistance to contamination and inhibition of carbon formation.
- Pore structure.
- Health and environmental impact.

3. Iron Oxides:

Due to its low cost and relatively high O_2 ability, Fe_2O_3 is the most common type of iron oxide investigated in the CLC process. Furthermore, iron oxides are less environmentally harmful than other metal oxides and have good potential for re-oxidation [4]. However, the use of hematite in CLC still faces challenges attributed to its thermodynamic limitations. Natural hematite is a non-permeable OC with a small surface area and a high risk of agglomeration when subjected to several high-temperature reaction cycles [5]. Substances such as alumina oxide (Al_2O_3), silica oxide (SiO_2), titanium dioxide (TiO_2) have also been studied for hematite. In the CLC processes, the most commonly used OC is Hematite; it is a readily available material [6, 7].

Pineau et al. suggested that two stages existed in the gas-fuelled reduction of hematite to wustite. i.e., hematite to magnetite and magnetite to wustite. It is also concluded that a compact iron layer formed during the reduction of Fe_2O_3 by H_2 at temperatures above 420°C. This compact iron layer was not present when CO was used. The reduction of Fe_2O_3 to Fe is thermodynamically limited.

Several iron-based OC has been tested for CLC applications. For continuous circulation systems using 20-100wt% Fe_2O_3, a few pilot studies range from 300 W_{th} to 10kW_{th} [8]. For a total of 40h service with natural gas and syngas as Fuel using 60wt% Fe_2O_3 on Al_2O_3 support, a test was conducted in a 300 W_{th} continuous unit at temperatures from 800 to 950 ° C[9]. There were no signs of OC deactivation, agglomeration, carbon formation, and little attrition. Noticed combustion efficiency of CH_4 was about 94%. During the 17h pilot test of iron-based OC with natural gas, Lyngfelt et al. identified 2-8 vol% CO in flue gas at lower fuel flow rates and higher OC circulation rates [10].

The solid-state reaction between Fe and Al_2O_3 appears to be the leading cause for loss of reactivity. $MgAl_2O_4$ is considered a support for iron to prevent the formation of $FeAl_2O_4$. This support increased reactivity and stability up to 1100°C. SiO_2 is not considered proper support for Fe_2O_3 due to its strong affinity to react with iron, which sharply reduces the reactivity [11].

4. Cobalt Oxides:

Cobalt (II) oxide (CoO), cobalt (III) oxide (Co_2O_3), or cobalt (II, III) oxide (Co_3O_4) may exist as cobalt oxides. Well-characterized and more stable than Co_2O_3 are CoO and CO_3O_4 [12]. Among these oxidized metals, the reduction of Co_3O_4 to Co-metal produces the most significant amount of O_2. For use in CLC, Co_3O_4 has many other benefits, such as a lower tendency for high-temperature sintering compared to other transition metal oxides. There is a greater capacity to carry O_2 and more significant reduction and re-oxidation rates [13].

It is also reported that when decreased by CH_4, cobalt oxides are more resistant to carbon deposition than nickel oxide. Due to the carcinogenic properties, Cobalt oxides are not considered for CLC processes [14].

As per thermodynamic findings, the metal oxide Co_3O_4 is a more reactive OC material for CH_4[5, 15]. This material has received relatively little attention for CLC applications due to its high cost compared to other transition metal oxides such as CuO [16].

The main disadvantage of this metal oxide is the tendency to decompose at comparatively low temperatures [5], resulting in less reactive CoO before reacting with CH_4. Hence the OC pair CoO/Co is considered for CLC units. Although it is thermodynamically favourable, 95—97% for H_2 and 87—97% for CO conversion is achieved between the temperature range of 800—1000°C [8]. Ryu et al. reported a 25h continuous operation in 50 kW_{th} CLC units on $COAl_2O_4$ with 99.6% conversion of CH_4 and concluded that attrition resistance of OC to be improved (26).

5. Copper Oxides:

CuO is relatively low in cost and exhibits high CH_4 reactivity [5, 8], thus having a reasonable regeneration rate. Furthermore, CuO reduction and re-oxidation are exothermic reactions, reducing the need for extra energy to drive these processes. However, CuO's use for CLC was restricted by CuO's low decomposition temperature, such as Co_3O_4, and its tendency to agglomerate [6].

Cao and colleagues found that CuO decomposed to Cu_2O at 600 ° C [17], although there was no evidence of agglomeration for the reacted particles. The idea of using a supported CuO has been discussed in several contributions. Indeed, there is more excellent stability for the supported CuO than bulk CuO. However, the configuration of the supported OC does not always equate to that of the unsupported carrier. Interaction of OC support material may lead to a robust metal-support interaction, limiting the amount of reducible phase in a supported OC[18].

Adanez et al. tested 15wt% CuO in 500 W_{th} and 10kW_{th} (120h of operation) CLC units with syngas and CH_4 as fuels. For an OC to fuel ratio >1.4 and temperature 800°C with 100% CH_4 conversion, no CO and H_2 emissions were noticed. Also, little and constant attrition of 0.04%/h was noticed for 50h of operation [19]. CuO decomposition to Cu_2O is possible at lower O_2 concentrations. Excess air in the AR is recommended to minimize CuO decomposition[20].

6. Nickel Oxide:

NiO has been widely investigated as an OC in bulk and supported forms. Bulk NiO's first reduction cycle shows good reactivity but low regeneration due to high agglomeration, decreasing reactivity and stability [21]. It is usually preferred to support NiO, with NiO / Al_2O_3 showing low particle agglomeration and high stability relative to bulk NiO [22, 23].

However, like with other metal oxide carriers, such as iron and copper oxides, the formation of non-reactive $NiAl_2O_4$ that restricts the performance of NiO / Al_2O_3 during CLC has been reported. By adding additional Ni, the excess NiO interacted with Al_2O_3 forming $NiAl_2O_4$, supplying enough additional NiO to serve as a stable OC.

$MgAl_2O_4$ as a support instead of Al_2O_3 was considered. The support of $MgAl_2O_4$ reducesthe sintering of NiO. As a result, the OC is stable over several redox cycles at a temperature > 1300°C. Ryden et al. opinionated that when NiO is used as an OC, combustion efficiency is limited to 99.4% at 950°C due to thermodynamic constraints[18].

7. Manganese oxides:

Manganese oxides are well known for reacting with CH_4, such as Mn_2, Mn_2O_3 and Mn_3O_4. MnO_2 decompose at 500°C. Only Mn_3O_4 is present at a temperature above 800°C. Therefore, the pair Mn_3O_4/MnO is only considered for CLC, restricting their use in CLC [5]. Mn_2O_3 is not stable at high temperatures, rendering it unacceptable for CLC[5].

Manganese oxides react with an inert material to form an irreversible un-reactive phase. Manganese Oxide OC with ZrO_2 inert stabilized with MgO showed good reactivity with syngas but lower reactivity for CH_4. During an investigation of continuous operating 300 W_{th} CLC at a temperature 800—950°C, higher efficiencies were observed for syngas than CH_4[24].

8. Thermodynamics:

Mattison et al. have conducted a thermodynamic analysis of different Redox pairs for a temperature range of 600—1200°C and plotted the values on log K and 1/T graph for CH_4 as fuel gas. Higher log K values are obtained for redox pairs MnO_2 / Mn_2O_3, Mn_2O_3/Mn_3O_4, Co_3O_4/CoO and CuO/Cu_2O.

In other words, these OC pairs have a higher affinity for CH_4. Few of the OC decomposes at a temperature such as MnO_2 (460°C), Mn_2O_3 (820°C), Co_3O_4 (890°C), and CuO (1030°C). With the possible exemption of CuO, other OCs are not suitable for CLC at higher temperatures[15].

II. MATERIAL AND METHODS

The following equations from (3) – (22) show different OCs reacting with CH_4 in Chemical Looping systems. The values in the parenthesis indicate the heat of reaction in kJ/mol.

$$4CdO + CH_4 \rightarrow 4Cd + CO_2 + 2H_2O\ (229.5) \quad \mathbf{(3)}$$

$$4CoO + CH_4 \rightarrow 4Co + CO_2 + 2H_2O\ (146.9) \quad \mathbf{(4)}$$

$$Co_3O_4 + CH_4 \rightarrow 3Co + CO_2 + 2H_2O\ (107.5) \quad \mathbf{(5)}$$

$$4Co_3O_4 + CH_4 \rightarrow 12CoO + CO_2 + 2H_2O\ (-10.5)\ \textbf{(6)}$$

$$4CuO + CH_4 \rightarrow 4Cu + CO_2 + 2H_2O\ (-173.5)\ \textbf{(7)}$$

$$8CuO + CH_4 \rightarrow 4Cu_2O + CO_2 + 2H_2O(-218.5)\ \textbf{(8)}$$

$$4Cu_2O + CH_4 \rightarrow 8Cu + CO_2 + 2H_2O\ (-128.1)\ \textbf{(9)}$$

$$4/3Fe_2O_3 + CH_4 \rightarrow 8/3Fe + CO_2 + 2H_2O\ (296.4)\ \textbf{(10)}$$

$$4Fe_2O_3 + CH_4 \rightarrow 8FeO + CO_2 + 2H_2O(318.3)\ \textbf{(11)}$$

$$12Fe_2O_3 + CH_4 \rightarrow 8Fe_3O_4 + CO_2 + 2H_2O(140.7)\ \textbf{(12)}$$

$$4/3In_2O_3 + CH_4 \rightarrow 8/3In + CO_2 + 2H_2O\ (431.8)\ \textbf{(13)}$$

$$4/3Mn_2O_3 + CH_4 \rightarrow 8/3Mn + CO_2 + 2H_2O(473.0)\ \textbf{(14)}$$

$$4Mn_2O_3 + CH_4 \rightarrow 8MnO + CO_2 + 2H_2O(-481)\ \textbf{(15)}$$

$$12Mn_2O_3 + CH_4 \rightarrow 8Mn_3O_4 + CO_2 + 2H_2O(-361)\ \textbf{(16)}$$

$$Mn_3O_4 + CH_4 \rightarrow 3Mn + CO_2 + 2H_2O(580.9)\ \textbf{(17)}$$

$$4Mn_3O_4 + CH_4 \rightarrow 12MnO + CO_2 + 2H_2O(108.7)\ \textbf{(18)}$$

$$4PbO + CH_4 \rightarrow 4PbO + CO_2 + 2H_2O(73.5)\ \textbf{(19)}$$

$$4NiO + CH_4 \rightarrow 4Ni + CO_2 + 2H_2O(157.5)\ \textbf{(20)}$$

$$4SnO + CH_4 \rightarrow 4Sn + CO_2 + 2H_2O(320.4)\ \textbf{(21)}$$

$$2SnO_2 + CH_4 \rightarrow 2Sn + CO_2 + 2H_2O(358.9)\ \textbf{(22)}$$

The enthalpy, entropy and Gibbs free energy of formation at 298K are obtained from HSC Chemistry10.0 software. The enthalpy of the reaction is calculated from Equation 23.

$$\Delta H° = \sum n_i * \Delta H_{i,product} - \sum n_i * \Delta H_{i,reacant}\ \textbf{(23)}$$

Where n_i is the stoichiometric coefficient of component “i” in the reaction, and H_i is the enthalpy of the component “$_i$” in the reaction.

Where $\Delta H_i°$ is calculated by

$$\Delta H° = \Delta H_{f,298.15K} + \int_{298.15}^{T} C_p\, dT\ \textbf{(24)}$$

The enthalpy of the reaction is calculated from Equation 25.

$$S = \sum n_i * S_{i,product} - \sum n_i * S_{i,reactant}\ \textbf{(25)}$$

$$S = S_{298.15K} + \int_{298.15}^{t} \frac{C_p}{T} dT\ \textbf{(26)}$$

Where n_i is the stoichiometric coefficient of component “$_i$” in the reaction and Si is the entropy of the component “i” in the reaction.

The Gibbs energy of the reaction is calculated from the following Equation 27.

$$\Delta G^{°} = \Delta H^{°} - T\Delta S\ \textbf{(27)}$$

Where T is the temperature at which reaction occurs. The equilibrium constant K is calculated from Equation 28.

$$K = e\text{^}((-H°/RT + \Delta S/R)\ )\ \textbf{(28)}$$

R is the universal gas constant of 8.314J/mol.K in the above equation. The forward rate constant to backward rate constant gives equilibrium constant (K), as shown in Equation 29.

$$K = k_{fwd\,/}k_{rev}\ \textbf{(29)}$$

When $k_{fwd}>>k_{rev}$, K is a large number ($>10^3$), and the concentration of products is predominant at equilibrium. The bigger number of the K corresponds to an irreversible reaction. Conversely, if $k_{fwd}<<k_{rev}$, K is smaller ($<10^{-3}$), the concentration of reactants at equilibrium predominate.

Systems for which $k_{fwd}<>k_{rev}$ have a significant concentration of products and reactants ($10^{-3}<K<10^3$).

A K value above 10^3 is considered a forward reaction for each reaction. If the value of K is less than $10^{-3,}$ thermodynamics favours reverse reaction. The reaction is at equilibrium for the K values between 10^{-3} and 10^3. The reaction temperatures that favour forward reaction are noted down.

1. Oxygen transport capacity:

Different OCs has different O_2 carrying capacities (R_o). The R_0 is the fraction of the weight of the total transferable O_2 when it is in a complete oxidized form in the OC. The Oxygen transport capacity can be calculated from Equation 30.

$$R_o = (m_{ox} - m_{red})/m_{ox} \quad \textbf{(30)}$$

Where m_{ox} is the mass of OC in the completely oxidized form and m_{re} is the mass of OC in the reduced form. The R_o is the function of the solids circulation rate describing the CLC unit, which will, in turn, affect the system's scale, configuration and efficiency of the reactor[6].

2. The extent of weight charge:

O_2 carrying capacity is described by converting O_2 to fully oxidized metal oxide relative to the total available O_2 or by the extent of the change in weight of the OC resulting from the conversion of O_2. The amount of O_2 converted varies linearly with the amount of change in the weight of the OC. The overall capacity of a metal oxide to transfer O_2 varies with metal and its oxidation states [3].

The gaseous species included in the calculation were CH_4, CO_2, CO, H_2O, H_2 and O_2, solid-phase metal oxides, and reduced metal oxides.

The degree of CH_4 yield to CO_2 defined as

$$\gamma_{red} = p_{co2}/(p_{CH4} + P_{CO2} + P_{CO}) \quad \textbf{(31)}$$

The enthalpy, entropy and Gibbs free energy of formation at 298K are obtained from HSC Chemistry10.0 software. The enthalpy of the reaction is calculated from Equation 23.

III. RESULTS AND DISCUSSION

1. Thermodynamics validation:

Fi displays Log (K) values for various redox pairs with 1/T. Log (K) and 1/T values are calculated using Equation 23-29. The result of these calculations is shown in Table 2. These results are truncated to the temperature range 600-1200°C. The Log (K) values compare with Mattisson and Lyngfelt [15].

Log(K) varies linearly with 1/T for a few redox pairs, notably Mn_2O_3/Mn_3O_4, Mn_2O_3/MnO, and all redox pairs, including Copper, as shown in Figure 2.

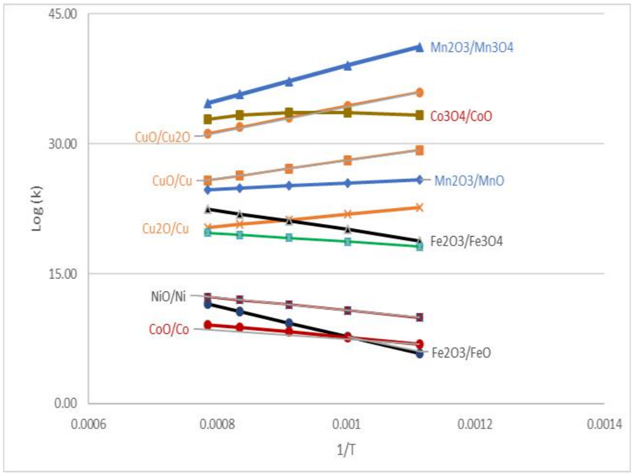

Fig 2. Log (K) Vs 1/T for various OC temperatures 600 -1200°C.

The log (k) value of other redox pairings varies inversely with 1/T. The redox pairs whose log (K) values vary linearly with 1/T are exothermic in FR reactions.

2. Detailed analysis of Thermodynamics:

2.1 Reaction temperature:

K values of each reaction have been calculated using equations 23 – 29. As mentioned in the previous section, K values $>10^3$favour forward reaction and $<10^{-3}$favour reverse reaction. Therefore, the minimum temperature of a reaction to a forward reaction is at which the K value is above 10^3. The forward temperature range for a few redox pairs is given in Table 1.

Few redox pairs such as copper oxides, Lead Oxides and Manganese Oxides can be reduced by CH_4 from a temperature of 298K. The Iron Oxides reduction starts at higher temperatures for Hematite to Iron and Hematite to Wustite. The reduction of Hematite to Magnetite starts from low temperatures (365K).

Oxides of Nickel and Cadmium transformation at medium temperature. In comparison, Tin Oxide will reduce at high temperatures. Cobalt Oxides appear to be reduced by CH_4 at medium temperatures. This analysis shows that the reaction of CH_4 with redox pairs Mn_2O_3/Mn, Mn_3O_4/Mn favour reverse reaction within the observed temperature range.

Based on this analysis, the order of affinity of redox pair with CH_4 is of the order Mn_2O_3/Mn_3O_4> CuO/Cu_2O > CuO/Cu > Cu_2O/Cu > Co_3O_4/CoO > Mn_2O_3/MnO > Fe_2O_3/Fe_3O_4>Mn_3O_4/MnO > PbO/Pb > Co_3O_4/Co > NiO/Ni > CdO/Cd > Fe_2O_3/FeO

>CoO/Co > SnO/SnO_2> SnO_2/Sn > Fe_2O_3/Fe > Mn_2O_3/Mn > Mn_3O_4/Mn.

2.2 Oxidation and reduction reactions:

Error! Reference source not found.gives the heat of reactions of various redox pairs with CH_4. Based on the data, the sum of the heat of reaction with each redox pair equals the heat of reaction of CH_4 combustion, which is -802.5 kJ/mol. The reduction reaction is always an endothermic reaction except for all copper oxides and a few manganese oxides pairs. For these pairs, reduction and oxidation are exothermic reactions.

The order in which these events occur (the difference between reduction and oxidation reactions) is the same as in Table 1.

2.3 Oxygen Carrying capacity (R_0):

R_0 is an essential characteristic of CLC. The mass conversion of OC (w) is calculated from R_0. Based on w, solid circulation rate and solid inventory are calculated[3].

O_2 carrying capacity of the studied redox pair follow the order Mn_2O_3/Mn > Fe_2O_3/Fe > Mn_3O_4/Mn > Co_3O_4/Co > NiO/Ni > CoO/Co > SnO_2/Sn > CuO/Cu > CdO/Cd> Cu_2O/Cu > Mn_2O_3/MnO > CuO/Cu_2O > Fe_2O_3/FeO > PbO/Pb > Mn_3O_4/MnO > Co_3O_4/CoO > Mn_2O_3/Mn3O4 > Fe_2O_3/Fe_3O_4.

Rate of O_2 transfer of a reduced metal oxide varies inversely with mass of reduced metal oxide. If the metal oxide mass flow rate of the reactant is higher, then O_2 transport capacity is lower.

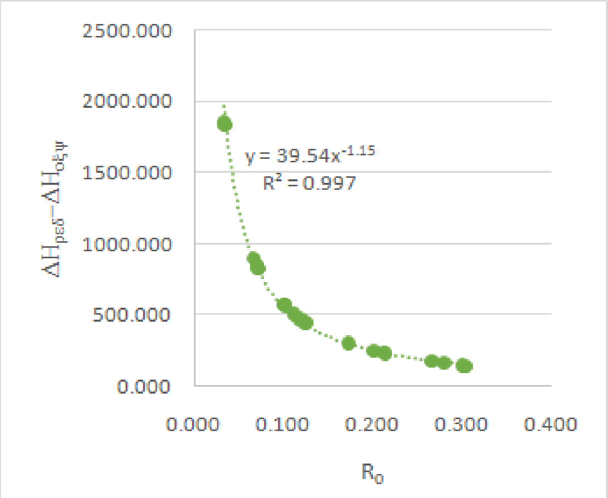

Fig 3. The relationship between ranges of heat of reaction with the O_2 carrying capacity of 20 redox pairs.

4. Cost of the metal for Oxygen Carrier:

The cost of the metal for various Oxygen Carrier is tabulated in Table-1. The cost of the metal is of the following order. Mn<Fe<Cd<Cu<Ni<Sn<In. These values are taken from daily metal prices based on December 2021 price.

It is also worth noting that for all redox pairs, the ratio of the sum of heat of reactions to the difference in mass of reduced and oxidised OCs is constant.

This statement is represented by equation (32).

$$(\Delta \boldsymbol{H}_{oxy} + \Delta \boldsymbol{H}_{red})/(\boldsymbol{m}_{red} - \boldsymbol{m}_{oxy}) = \boldsymbol{k} \quad \mathbf{(32)}$$

The value of K is found to be -12.04 for all twenty redox pairs. The difference in the mass of reduced and oxidised OC is the mass of O_2 transported between OC.

2.4 The extent of conversion:

Extension of conversion is of the order CuO/Cu > Fe_2O_3/Fe > NiO/Ni > Mn_2O_3/Mn > Mn_3O_4/Mn > CuO/Cu_2O > Cu_2O/Cu > Fe_2O_3/FeO > Mn_2O_3/MnO > Mn_3O_4/MnO > Fe_2O_3/Fe_3O_4> Mn_2O_3/Mn_3O_4.

3. Activation energy:

The plot slope obtained from ln(k) vs 1/T is -Ea/R. These values are displayed in Fig, along with the enthalpy of formation for various redox pairs. Higher the enthalpy of formation, higher activation energy is required.

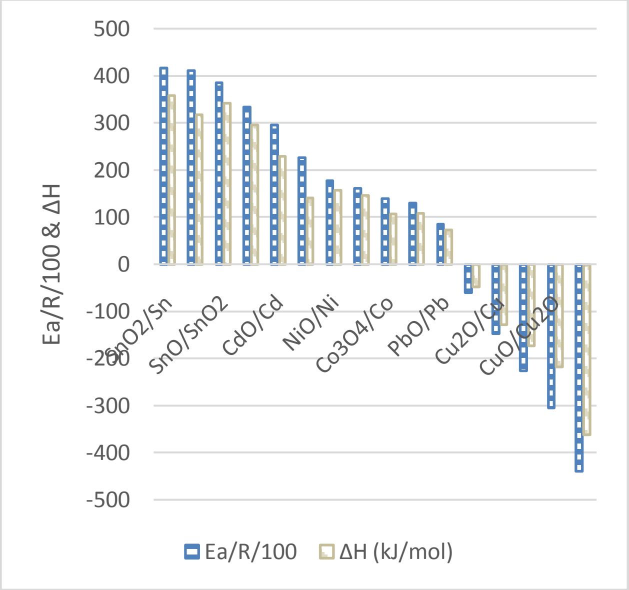

Fig 4. Comparison between Enthalpy of formation and Ea/R for various OC and CH_4 reactions.

The order of activation energy for the forward reaction of CH_4 for various metal oxides is of the order SnO_2/Sn > Fe_2O_3/FeO > Fe_2O_3/Fe > CdO/Cd > Fe_2O_3/Fe_3O_4> NiO/Ni > CoO/Co > Co_3O_4/Co > Mn_3O_4/MnO > PbO/Pb > Mn_2O_3/MnO > Cu_2O/Cu > CuO/Cu > CuO/Cu_2O > Mn_2O_3/Mn_3O_4.

IV. CONCLUSION

The thermodynamics of various OC reductions by CH_4 in the FR were thoroughly investigated using HSC Chemistry V10.0. The temperature range for this analysis is 298.15—1273.15K.The minimum temperature required to reduce OC by CH_4 for forwarding reaction to produce CO_2 and H_2O is determined. The minimum temperature required for a forward reaction is calculated on the K value of the reaction. For a reaction to favour products, the K value shall be above 1.0^{03}.

In the analysis, it is noticed that, for a temperature range of 600—1200K, the redox pairs whose log (K) values vary linearly with 1/T are exothermic in the FR reactions.

The sum of heat of reactions to the difference in mass of reduced and oxidized OCs is constant for all redox pairs participating in CLC processes. The activation energy for the forward reaction is calculated by finding the slope of Log(K) vs 1/T for various OC with fuel CH_4. Activation energy varies linearly with enthalpy of formation. OC pairs are categorized based on O_2 transport capabilities and the maximum extent of conversion. In future work, a thermodynamic analysis with syngas will be considered.

V. ACKNOWLEDGEMENTS

The authors would like to acknowledge the contribution of an Australian Government Research Training Program Scholarship in supporting this research.

REFERENCES

[1] Abad et al. (2007). Mapping of the range of operational conditions for Cu-, Fe-, and Ni-based oxygen carriers in chemical-looping combustion. Chemical Engineering Science, 62, 533—549. https://doi.org/10.1016/j.ces.2006.09.019.

[2] P.-C. Chiu and Y. Ku. (2012). Chemical Looping Process – A novel Technology for inherent CO2 capture, Aerosol and Air Quality Research, 12, 1421—1432.doi: 10.4209/aaqr.2012.08.2015.

[3] L.-S. Fan and L.-S. Fan (2010). Chemical Looping Systems for Fossil Energy Conversions. Hoboken, UNITED STATES: American Institute of Chemical Engineers, 2010.

[4] D. Wen, P. Song, K. Zhang, and J. Qian (2011). Thermal oxidation of iron nano-particles and its implication for chemical-looping combustion. Journal of Chemical Technology & Biotechnology, 86, 375-380. doi: https://doi.org/10.1 002/jctb.2526.

[5] M. M. Hossain and H. I. de Lasa (2008). Chemical-looping combustion (CLC) for inherent CO2 separations—a review. Chemical Engineering Science, 63, 4433-4451. https://doi.org/10.1016/j.ces.2008.05.028.

[6] Z. Yu et al. (2019). Iron-based oxygen carriers in chemical looping conversions: A review.Carbon Resources Conversion, 2, 23-34.doi: https://doi.org/10.1016/j.crcon.2018.11.004.

[7] A. Pineau, N. Kanari, and I. Gaballah (2006). Kinetics of reduction of iron oxides by H2: Part I: Low temperature reduction of hematite. Thermo chimica Acta, 447, 89-100. https://doi.org/10.1016/j.tca.2005.10.004.

[8] J. Li, H. Zhang, Z. Gao, J. Fu, W. Ao, and J. Dai (2017). CO2 Capture with Chemical Looping Combustion of Gaseous Fuels: An Overview. Energy & Fuels, 31, 3475-3524. doi: 10.1021/a

cs.energyfuels.6b03204.

[9] A. Abad, T. Mattisson, A. Lyngfelt, and M. Johansson (2007). The use of iron oxide as oxygen carrier in a chemical-looping reactor.Fuel, 86, 1021-1035. doi: https://doi.org/10.1016/j.fuel.2006.09.021.

[10] Lyngfelt A, Thunman H (2005). Construction and 100 h of Operational Experience of A 10-kW Chemical-Looping Combustor. Carbon Dioxide Capture Storage Deep Geol Form, 1,625–45. https://doi.org/10.1016/B978-008044570-0/50122-7.

[11] Q. Zafar, T. Mattisson, and B. Gevert (2006). Redox Investigation of Some Oxides of Transition-State Metals Ni, Cu, Fe, and Mn Supported on SiO2 and MgAl2O4,. Energy & Fuels, 20, 34-44.doi: 10.1021/ef0501389.

[12] S. C. Petitto, E. M. Marsh, G. A. Carson, and M. A. Langell (2008). Cobalt oxide surface chemistry: The interaction of CoO(100), Co3O4(110) and Co3O4(111) with Oxygen and water. Journal of Molecular Catalysis A: Chemical, 281,49-58.https://doi.org/10.1016/j.molcata.2007.08.023.

[13] K. Wang, Q. Yu, Q. Qin, and W. Duan (2014). Feasibility of a Co Oxygen Carrier for Chemical Looping Air Separation: Thermodynamics and Kinetics. Chemical Engineering & Technology, 37, 1500-1506. doi: https://doi.org/10.1002/ceat.201400178.

[14] Q. Imtiaz, D. Hosseini, and C. R. Müller (2013). Review of Oxygen Carriers for Chemical Looping with Oxygen Uncoupling (CLOU): Thermodynamics, Material Development, and Synthesis. Energy Technology, 1, 633-647.

[15] doi: https://doi.org/10.1002/ente.201300099.

[16] T. Mattisson and A. Lyngfelt (2001). Capture of CO2 Using Chemical-Looping Combustion. First Biennial Meeting of the Scandinavian-Nordic Section of the Combustion Institute.

[17] C. Fu and P. S. Grant (2015). Toward Low-Cost Grid Scale Energy Storage: Super capacitors Based on Up-Cycled Industrial Mill Scale Waste. ACS Sustainable Chemistry & Engineering, 3, 2831-2838. doi: 10.1021/acssuschemeng.5b00757.

[18] Y. Cao, B. Casenas, and W.-P. Pan (2006). Investigation of Chemical Looping Combustion by Solid Fuels. 2. Redox Reaction Kinetics and Product Characterization with Coal, Biomass, and Solid Waste as Solid Fuels and CuO as an Oxygen Carrier. Energy & Fuels, 20, 1845-1854. doi: 10.1021/ef050424k.

[19] M. Rydén, M. Johansson, A. Lyngfelt, and T. Mattisson (2009). NiO supported on Mg–ZrO2 as oxygen carrier for chemical-looping combustion and chemical-looping reforming. Energy & Environmental Science,. 2, doi: 10.1039/b904370e.

[20] J. Adánez, P. Gayán, J. Celaya, L. F. de Diego, F. García-Labiano, and A. Abad (2006).Chemical Looping Combustion in a 10 kWth Prototype Using a CuO/Al2O3 Oxygen Carrier: Effect of Operating Conditions on Methane Combustion. Industrial & Engineering Chemistry Research, 45, 6075-6080. doi: 10.1021/ie060364l.

[21] L. F. de Diego et a;. (2007). Operation of a 10kWth chemical-looping combustor during 200h with a CuO–Al2O3 oxygen carrier. Fuel, 86, 1036-1045. doi: https://doi.org/10.1016/j.fuel.2006.10.004.

[22] H. Jin and M. Ishida (2004). A new type of coal gas fueled chemical-looping combustion. Fuel, 83, 2411-2417. doi: https://doi.org/10.1 016/j.fuel.2004.06.033.

[23] H. Jin and M. Ishida (2000). A novel gas turbine cycle with hydrogen-fueled chemical-looping combustion. International Journal of Hydrogen Energy, 25, 1209-1215. doi: https://doi.org/10.1016/S0360-3199(00)00032-X.

[24] H. Jin and M. Ishida (2001). Reactivity study on a novel hydrogen fueled chemical-looping combustion. International Journal of Hydrogen Energy, 26, 889-894. doi: https://doi.org/10.1016/S0360-3199(01)00015-5.

[25] A. Lyngfelt, B. Leckner, and T. Mattisson (2001). A fluidised-bed combustion process with inherent CO2 separation; application of chemical-looping combustion. Chemical Engineering Science, 56, 3101-3113. doi: https://doi.org/10.1016/S0009-2509(01)00007-0.

[26] J. Hu, V. V. Galvita, H. Poelman, and G. B. Marin (2018). Advanced Chemical Looping Materials for CO2 Utilization: A Review. Materials, 11, 1187, https://www.mdpi.com/1996-1944/11/7/1187.

[27] Ryu, H.-J.; Jo, S.-H.; Park, Y. C.; Bae, D.-H.; Kim, S. (2010). Long term operation experience in a 50 kWth chemical looping combustor using natural gas and syngas as fuels. Proceedings of the 1st International Conference on Chemical Looping,